

EXHIBIT
Kille

849

1N-71

325153

P.49

NASA
Technical
Paper
3057
DOE/NASA/
20320-77

December 1990

166
Wind Turbine Acoustics

Harvey H. Hubbard
and Kevin P. Shepherd

Work performed for
U.S. Department of Energy
Wind/Hydro/Ocean Technologies Division
and
Solar Energy Research Institute
Solar Technology Information Program

(NASA-TP-3057)
(NASA) 49 p

WIND TURBINE ACOUSTICS
CSCL 20A

N91-16679

Unclas
H1/71 0325153



understood factors is the effect of the wind. Included here are brief discussions of the effects of distance from various types of sources, the effects of such atmospheric factors as absorption in air and refraction caused by sound speed gradients, and terrain effects.

Distance Effects

Point Sources

When there is a nondirectional point source as well as closely grouped, multiple point sources, spherical spreading may be assumed in the far radiation field. Circular wave fronts propagate in all directions from a point source, and the sound pressure levels decay at the rate of -6 dB per doubling of distance in the absence of atmospheric effects. The latter decay rate is illustrated by the straight line in Figure 7-18. The dashed curves in the figure represent increased decay rates associated with atmospheric absorption at frequencies significant for wind turbine noise.

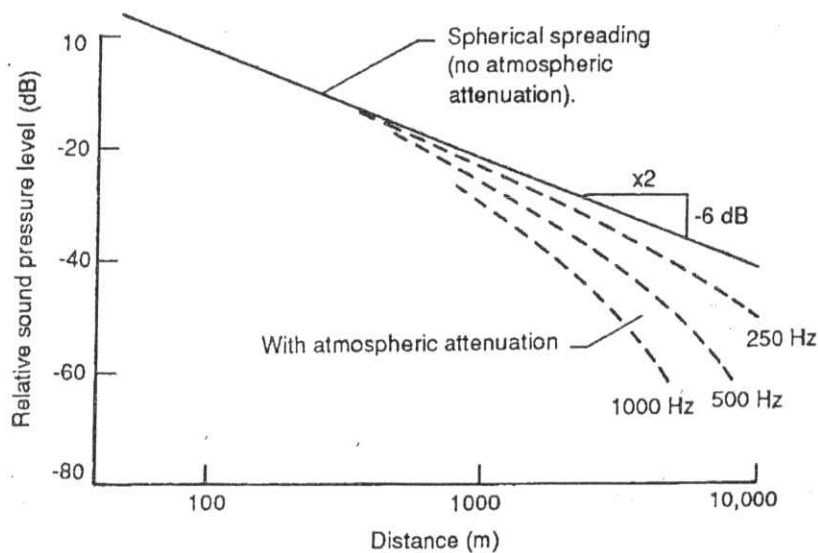


Figure 7-18. Decrease in sound pressure levels of pure tones as a function of distance from a point source [ANSI 1978]

Line Sources

For an infinitely long line source, the decay rate is only -3 dB per doubling of distance, compared with the -6 dB per doubling of distance illustrated in Figure 7-18. Such a reduced decay rate is sometimes observed for sources such as trains and lines of vehicles on a busy road. Some arrays of multiple wind turbines in wind power stations may also behave acoustically like line sources.

Atmospheric Factors

Absorption in Air

As sound propagates through the atmosphere, its energy is gradually converted to heat by a number of molecular processes such as shear viscosity, thermal conductivity, and molecular relaxation, and thus atmospheric absorption occurs. The curves in Figure 7-19 were plotted from ANSI values [1978] and show changes in atmospheric absorption as a function of frequency. In these examples, the ambient temperature varied from 0° to 20°C and the relative humidity varied from 30% to 70%. The atmospheric absorption is relatively low at low frequencies, increasing rapidly as a function of frequency. Atmospheric absorption values for other conditions of ambient temperature and relative humidity can be obtained from the ANSI tables; these values follow the general trend shown in Figure 7-19.

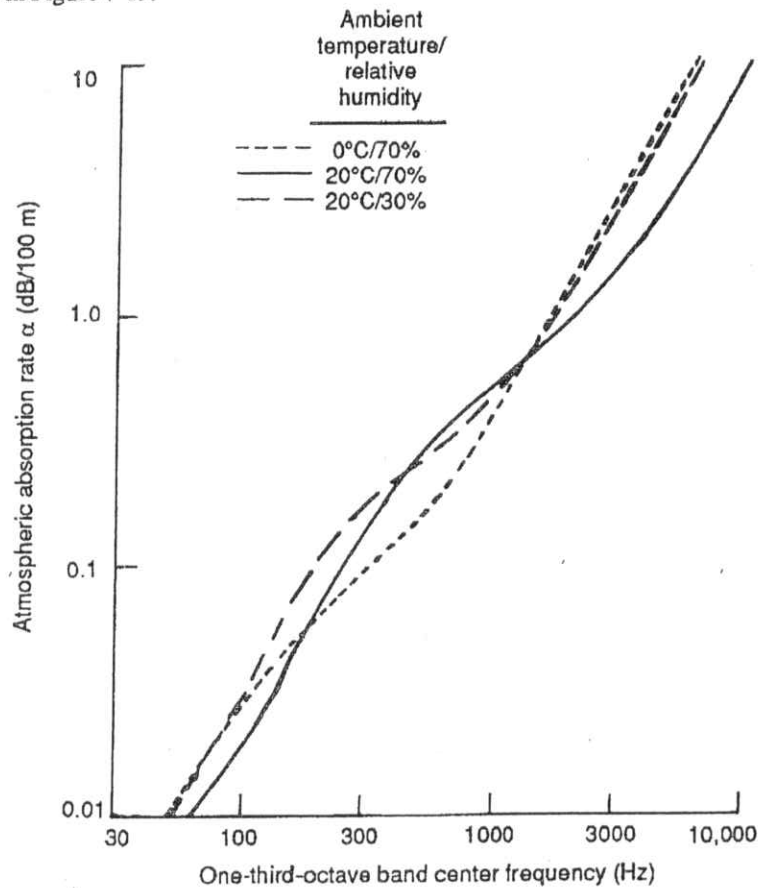


Figure 7-19. Standard rates of atmospheric absorption [ANSI 1978]

Refraction Caused by Wind and Temperature Gradients

Refraction effects arising from the sound speed gradients caused by wind and temperature can cause nonuniform propagation as a function of azimuth angle around a source. Figure 7-20 is a simple illustration of the effects of atmospheric refraction, or bending of

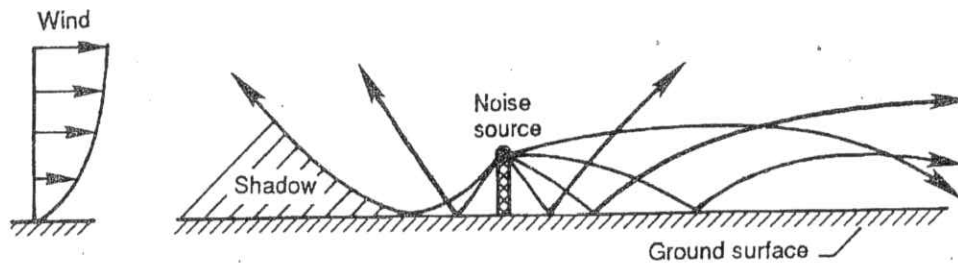


Figure 7-20. Effects of wind-induced refraction on acoustic rays radiating from an elevated point source [Shepherd and Hubbard 1985]

sound rays, caused by a vertical wind-shear gradient over flat, homogeneous terrain for an elevated point source. Note that in the downwind direction the wind gradient causes the sound rays to bend toward the ground, whereas in the upwind direction the rays curve upward away from the ground. For high-frequency acoustic emissions, this causes greatly increased attenuation in a shadow zone upwind of the source, but little effect downwind. The attenuation of low-frequency noise, on the other hand, is reduced by refraction in the downwind direction, with little effect upwind.

The distance from the source to the edge of the shadow zone is related to the wind-speed gradient and the elevation of the source. In a 10- to 15-m/s wind, for a source height from 40 to 120 m above flat, homogeneous terrain, the horizontal distance from the source to the shadow zone was calculated to be approximately five times the height of the source [Shepherd and Hubbard 1985].

Attenuation exceeding that predicted by spherical spreading and atmospheric absorption can be found in the shadow zone. This attenuation is frequency-dependent, and the lowest frequencies are the least attenuated. Figure 7-21 presents an empirical scheme for estimating attenuation in the shadow zone, based on information in Piercy, Embleton, and Sutherland [1977]; SAE [1966]; and Daigle, Embleton, and Piercy [1986]. The estimated

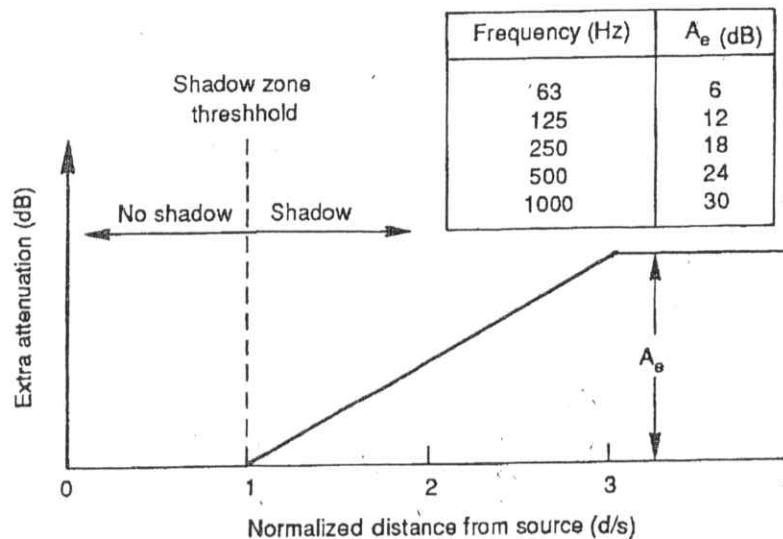


Figure 7-21. Empirical model for estimating the extra attenuation of noise in the shadow zone upwind of an elevated point source ($s = 5h$, $40 \leq h \leq 120$ m, where h = source elevation) [Shepherd and Hubbard 1985]

extra attenuation (A_e in Figure 7-21) is assumed to take place over a distance equal to twice that from the source to the edge of the shadow zone. The predicted decay in the sound pressure level from the source to the edge of the shadow zone is caused by atmospheric absorption [ANSI 1978] and spherical spreading. Within the shadow zone, extra attenuation should be added as estimated according to Figure 7-21.

Note that vertical temperature gradients, which are also effective sound speed gradients, will normally also be present. These will add to or subtract from the effects of wind that are illustrated in Figure 7-21. Effects of wind gradient will generally dominate those of temperature gradients in noise propagation from wind power stations.

Distributed Source Effects

Because of their large rotor diameters, some wind turbines exhibit distributed source effects relatively close to the machines. Only when listeners are at distances from the turbines that are large in relation to the rotor diameter does the rotor behave acoustically as a point source. As indicated in Figure 7-22, distributed source effects are particularly important in the upwind direction. In this figure, sound pressure levels in the 630-Hz, one-third-octave band are presented as a function of distance in the downwind, upwind, and crosswind directions. The measured data agree well with the solid curves, which represent spherical spreading and atmospheric absorption in the downwind and crosswind directions. In the upwind direction, however, the measured data fall below the solid curve; this

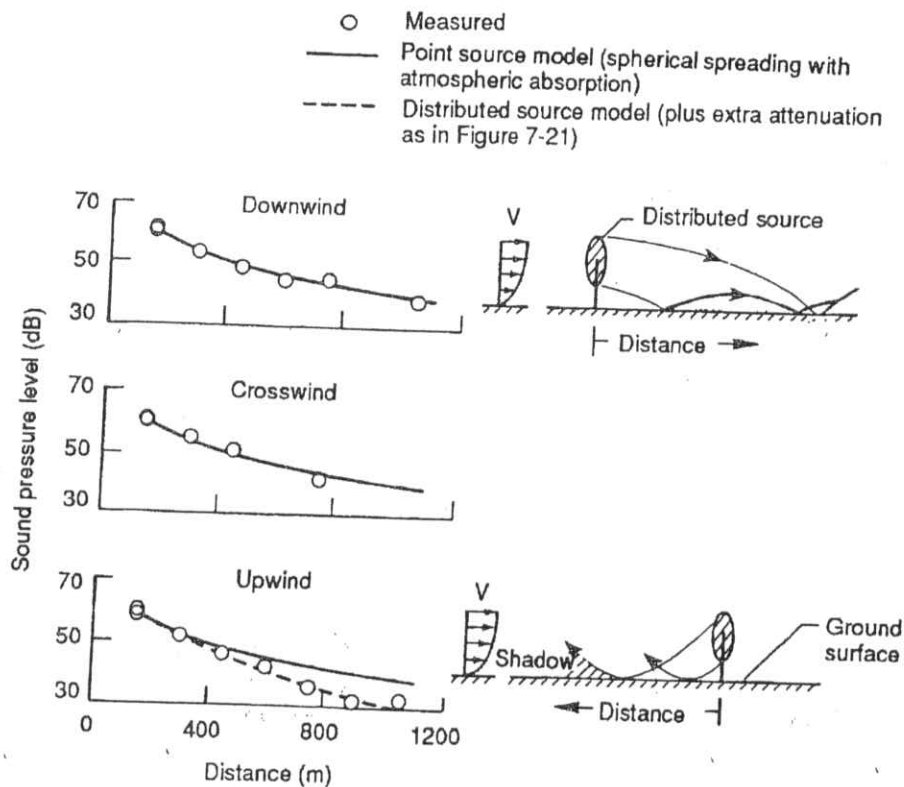


Figure 7-22. Measured and calculated sound pressure levels in three directions from a large-scale HAWT (one-third-octave band = 630 Hz, rotor diameter = 78.2 m) [Shepherd and Hubbard 1985]

indicates the presence of a shadow zone. An improvement in predicting upwind sound pressure levels is obtained when the noise source is modeled as being distributed over the entire rotor disk. Each part of the disk is then considered to be a point source, and attenuation is estimated by means of the empirical model shown in Figure 7-21. The resulting predictions are shown as the dashed curve of Figure 7-22 and are in good agreement with the sound measurements upwind of the turbine. In the downwind and crosswind directions, point-source and distributed-source models result in identical calculations of sound pressure levels.

Channeling Effects at Low Frequencies

Figure 7-23 illustrates the special case of propagation of low-frequency rotational-harmonics when the atmospheric absorption and extra attenuation in the shadow zone are very small. Measured sound pressure levels are shown as a function of distance for both the upwind and downwind directions. For comparison, the curves representing decay rates of -6 dB and -3 dB per doubling of distance are also included. Note that in the upwind case the sound pressure levels tend to follow a decay rate of -6 dB per doubling of distance, which is equal to the rate for spherical spreading. No extra attenuation from a shadow zone was measured.

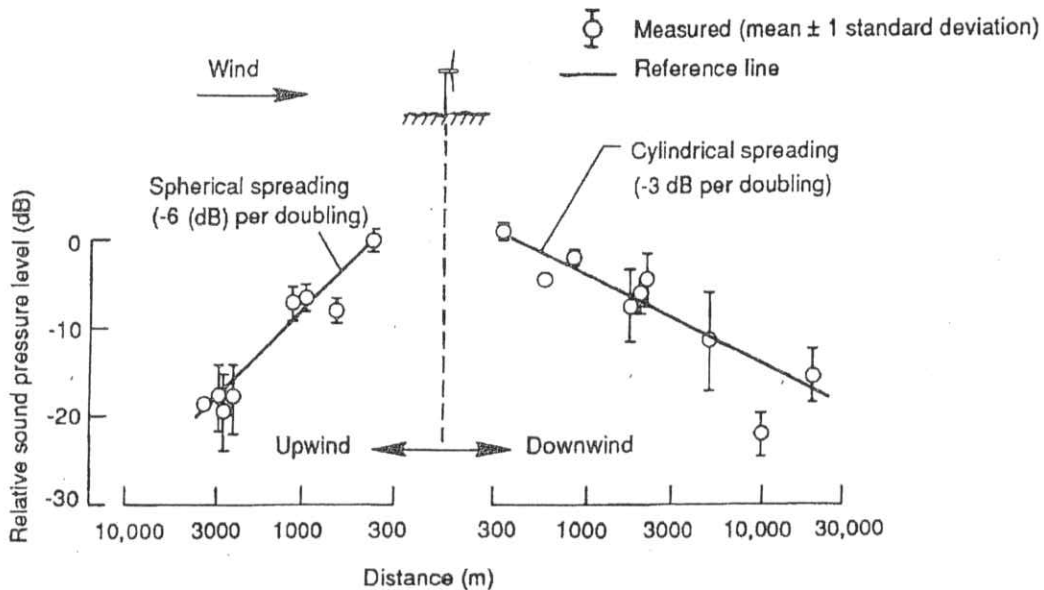


Figure 7-23. Measure effect of wind on the propagation of low-frequency rotational harmonic noise from a large-scale HAWT (harmonics with frequencies from 8 to 16 Hz, rotor diameter = 78.2 m) [Willshire and Zorumski 1987]

In the downwind direction, the sound pressure levels tend to follow a decay rate of -3 dB per doubling of distance, similar to that for cylindrical spreading. This reduced decay rate in the downwind direction at very low frequencies is believed to result from atmospheric refraction, which introduces a channeling sound path in the lower portions of the earth's boundary layer [Willshire and Zorumski 1987; Thomson 1982; Hawkins 1987].

Terrain Effects

Terrain effects include ground absorption, reflection, and diffraction. Furthermore, terrain features may cause complex wind gradients, which can dominate noise propagation to large distances [Kelley *et al.* 1985; Thompson 1982]. Wind turbines are generally located in areas devoid of trees and other large vegetation. Instead, ground cover usually consists of grass, sagebrush, plants, and low shrubs, which are minor impediments to noise propagation except at very high frequencies. At frequencies below about 1000 Hz, the ground attenuation is essentially zero.

Methods are available for calculating the attenuations provided by natural barriers such as rolling terrain, which may interrupt the line of sight between the source and the receiver [Piercy and Embleton 1979]. However, very little definitive information is available regarding the effectiveness of natural barriers in the presence of strong, vertical wind gradients. Piercy and Embleton [1979] postulate that the effectiveness of natural barriers in attenuating noise is not reduced under conditions of upward-curving ray paths (as would apply in the upwind direction) or under normal temperature-lapse conditions. However, under conditions of downward-curving ray paths, as in downwind propagation or during temperature inversions (which are common at night), the barrier attenuations may be reduced significantly, particularly at large distances.

Predicting Noise from Multiple Wind Turbines

Methods are needed to predict noise from wind power stations made up of large numbers of machines, as well as for a variety of configurations and operating conditions. This section reviews the physical factors involved in making such predictions and presents the results of calculations that illustrate the sensitivity of radiated noise to various geometric and propagation parameters. A number of valid, pertinent, simplifying assumptions are presented. A logarithmic wind gradient is assumed, with a wind speed of 9 m/s at hub height. Flat, homogeneous terrain, devoid of large vegetation, is also assumed. Noises from multiple wind turbines are assumed to add together incoherently, that is, in random phase.

Noise Sources and Propagation

Reference Spectrum for a Single Wind Turbine

The most basic information needed to predict noise from a wind power station is the noise output of a single turbine. Its noise spectrum can be predicted from knowledge of the geometry and operating conditions of the machine [Viterba 1981; Glegg, Baxter, and Glendinning 1987; Grosveld 1985], or its spectrum can be measured at a reference distance. Figures 7-9 and 7-10 are examples of spectral data for HAWTs. Also shown in Figure 7-10 is a hypothetical spectrum used in subsequent example calculations to represent a HAWT with a 15-m rotor diameter and a rated power of approximately 100 kW. The example spectrum is the solid line with a decrease of 10 dB per decade in sound pressure level with increasing frequency. This spectral shape is generally representative of the aerodynamic noise radiated by wind turbines. However, predictions for a specific wind power station should be based, if possible, on data for the particular types of turbines in the station.

Directivity of the Source

Measurements of aerodynamic noise for a number of large HAWTs (for example, Kelley *et al.* [1985]; Hubbard and Shepherd [1982]; and others listed in the bibliography) indicate that the source directivity depends on specific noise-generating mechanisms. For broadband noise sources, such as inflow turbulence and interactions between the blade boundary layer and the blade trailing edge, the sound pressure level contours at close distances are approximately circular. Lower-frequency, impulsive noise, which results when the blades interact with the tower or central column wake, radiates most strongly in the upwind and downwind directions.

Although there is one prevailing wind direction at most wind turbine sites, it is not uncommon for the wind vector to vary 90° in azimuth angle during normal operations. Therefore, one of the simplifying assumptions made in the calculations that follow is that each individual machine behaves like an omnidirectional source.

Considerations for Frequency Weighting

A-weighted sound pressure levels, expressed in dB(A), are in widespread use in evaluating the effects of noise on communities [Pearsons and Bennett 1974]. Figure 7-24 shows the results of applying this descriptor. The assumed single-turbine reference spectrum, at a distance of 30 m from the machine, is reproduced from Figure 7-10 as the solid line. The equivalent A-weighted spectrum at the same distance is shown as the upper dashed curve. This particular weighting emphasizes the higher frequencies and deemphasizes the lower frequencies according to the sensitivity of the human ear. As distances increase, as illustrated in the other dashed curves, atmospheric absorption causes the levels of the higher-frequency components to decay faster than those of the lower frequencies (see Figure 7-19). The result is that the midrange frequencies (100 to 1000 Hz) tend to dominate the A-weighted spectrum at large distances. Frequencies higher than 1000 Hz will generally not be important considerations at large distances because of the effects of atmospheric absorption. Frequency components below about 100 Hz may not be

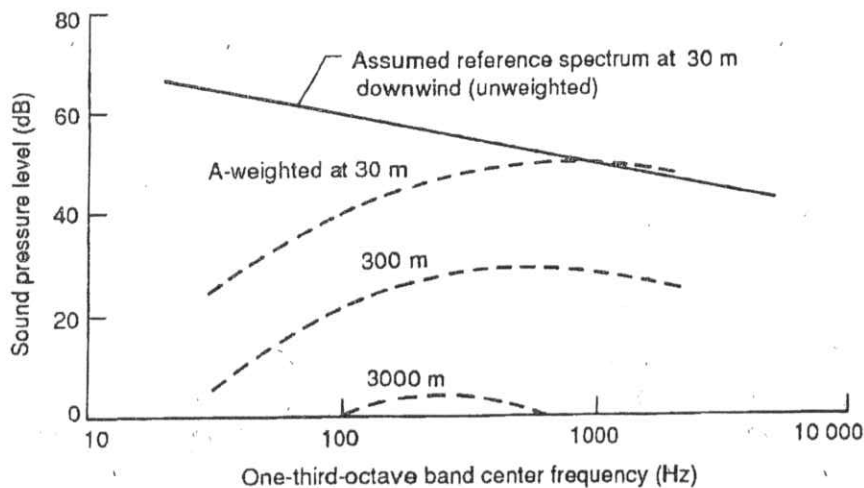


Figure 7-24. Reference and A-weighted noise spectra from a 15-m-diameter HAWT with a rated power of 100 kW (assumed for example calculations of noise from a wind power station)

significant in terms of audible noise, but they can be significant in terms of such indirect effects as noise-induced building vibrations.

Arrangement of Wind Power Stations

A basic geometric arrangement of wind turbines was assumed to represent an example wind power station (shown in Figure 7-25). The station consists of 31 turbines per row. Each machine produces approximately 100 kW of power, and the rotor diameter is 15 m. The spacing between turbines is 30 m, the row length is 900 m, and the spacing between rows is 200 m. The basic four-row configuration in Figure 7-25 was perturbed to investigate the effects of such variables as the number of rows, row and turbine spacing, row length, and turbine power rating.

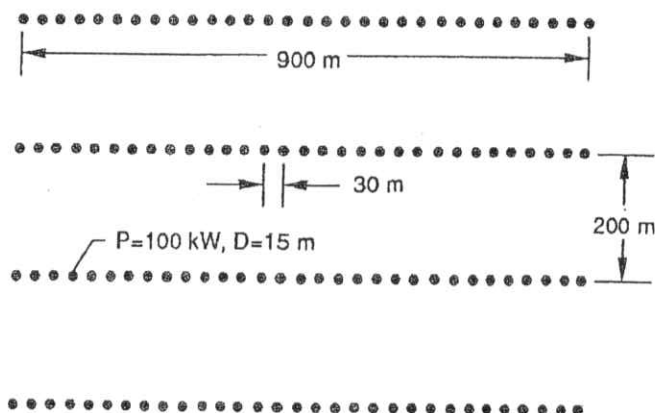


Figure 7-25. Layout of wind turbines in the example wind power station [Shepherd and Hubbard 1986]

Absorption and Refraction

These example calculations assumed an ambient temperature of 20°C and a relative humidity of 70%. From the data in Figure 7-19, assumed values of atmospheric absorption of 0, 0.10, 0.27, and 0.54 dB per 100 m correspond roughly to one-third-octave band center frequencies of 50, 250, 500 and 1000 Hz, respectively, for these temperature and humidity conditions. These frequencies were chosen because they encompass the range of frequencies considered important in evaluating the perception of wind turbine noise in adjacent communities [Shepherd and Hubbard 1986].

Calculation Methods

The method presented here for calculating the sound pressure level from incoherent addition is a sum of the random-phase multiple noise sources at any arbitrary receiver distance. This method assumes that each source radiates equally in all directions. Attenuation caused by atmospheric absorption is included; propagation is over flat, homogeneous terrain; and there is a logarithmic wind-speed gradient. The method has no limitations on the number of wind turbines or their geometric arrangements. The required input is a reference sound-pressure-level spectrum $L_p(f)$, either narrow-band or one-third-octave band,

for a single wind turbine. This spectrum can be measured or predicted for a reference distance from the rotor hub of approximately 2.5 times the rotor diameter.

The sound pressure level received from an individual wind turbine in the array in a given frequency band can be calculated with the following equation:

$$L_n(f_i) = L_o(f_i) - 20 \log_{10} (d_n/d_o) - \alpha(d_n - d_o)/100 \quad (7-8)$$

where

- $L_n(f_i)$ = sound pressure level from the nth wind turbine (dB)
- n = wind turbine index (1, 2, ..., N)
- N = number of wind turbines in the array
- f_i = center frequency of the ith band (Hz)
- $L_o(f_i)$ = reference sound pressure level in the ith frequency band from a single wind turbine at the reference distance (dB)
- d_n = distance from the nth turbine to the receiver (m)
- d_o = reference turbine-to-receiver distance (m)
- α = atmospheric absorption rate (dB per 100 m)

The total sound pressure level, from all wind turbines in the array in the ith frequency band, is then calculated as follows:

$$SPL_{tot}(f_i) = 10 \log_{10} \sum_n 10^{L_n(f_i)/10} \quad (7-9)$$

This procedure can be repeated for all frequency bands to provide a predicted spectrum of sound pressure level at the receiver location. Noise measures such as the A-weighted sound pressure level may also be calculated by adding the A-weighting corrections at each frequency to the values of $L_n(f_i)$ or $SPL_{tot}(f_i)$ in Eqs. 7-8 and 7-9. If the sources are arranged in rows, the required computations can be reduced by using the simplified procedures of Shepherd and Hubbard [1986].

Examples of Calculated Noise for Wind Power Stations

A series of parametric calculations of unweighted sound pressure levels was performed based on the array of Figure 7-25 and systematic variations of that array [Shepherd and Hubbard 1986]. The receiver is assumed to be on a line of symmetry either in the downwind, upwind, or crosswind direction.

Effect of Distance from a Single Row

Figure 7-26 shows calculated sound pressure levels for one row of the example wind power station, as a function of downwind distance for various rates of atmospheric absorption. Also shown are reference decay rates of -3 dB and -6 dB per doubling of distance. For an atmospheric absorption rate of zero, the decay rate is always less than that for a single point source (Figure 7-18). At intermediate distances, the row of turbines acts as a line source, for which the theoretical decay rate is -3 dB per doubling of distance or -10 dB per decade of distance. Only at distances greater than one row length (900 m) does the decay rate approach the single-point-source value of -6 dB per doubling of distance (-20 dB per decade). Decay rates increase as the absorption coefficient increases.

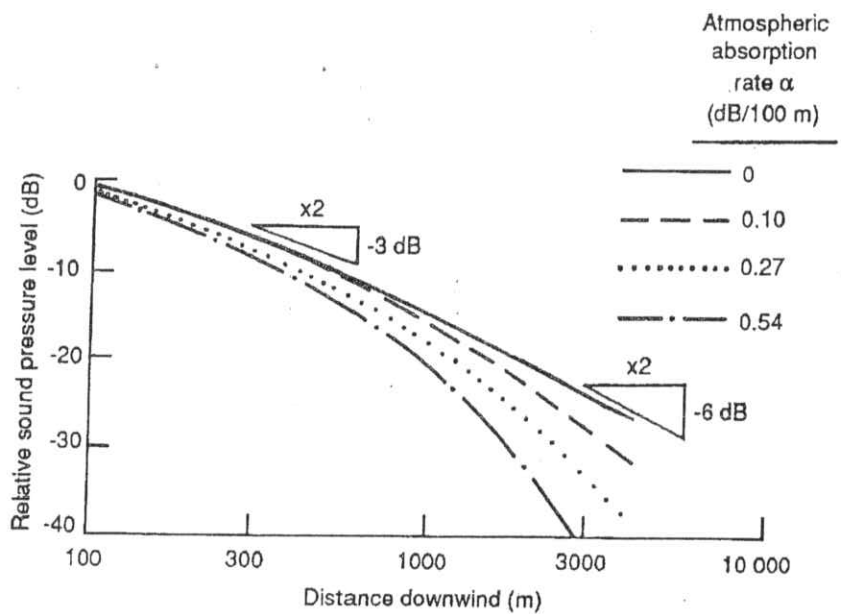


Figure 7-26. Calculated noise propagation downwind of a single row of wind turbines in the example array for four atmospheric absorption rates [Shepherd and Hubbard 1986]

Effect of Multiple Rows

Figure 7-27 presents the results of sound-pressure-level calculations that were made for one, two, four, and eight rows of wind turbines; this illustrates the effects of progressively doubling the number of machines for a constant turbine spacing. At zero atmospheric absorption, and at receiver distances that are large relative to the array dimensions, a doubling of the number of rows results in an increase of 3 dB in the sound pressure level.

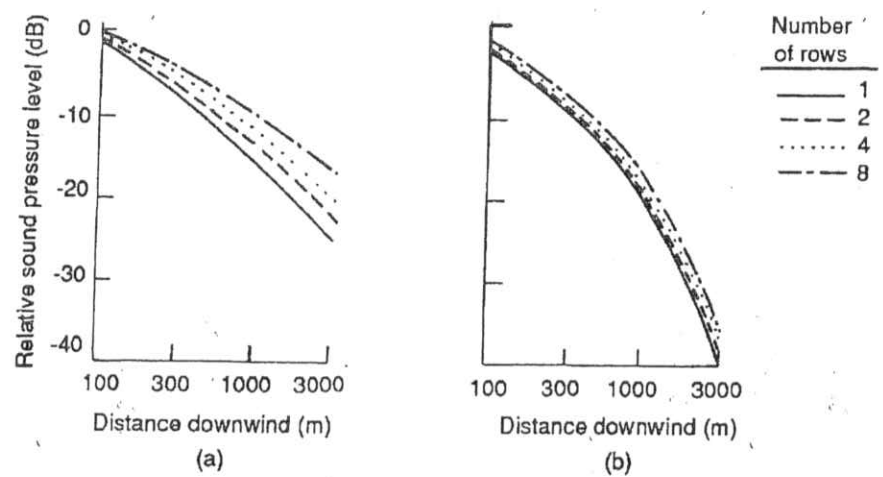


Figure 7-27. Calculated noise propagation downwind of various numbers of rows of wind turbines in the example array [Shepherd and Hubbard 1986]. (a) without atmospheric absorption. (b) $\alpha = 0.54$ dB/100 m.

This simply reflects a doubling of acoustic power. At shorter distances, the closest machines dominate and the additional rows result in only small increments in the sound pressure level.

For nonzero atmospheric absorption, the effect of additional rows is less significant at all receiver distances. Doubling the number of rows results in an increase in the sound pressure level of less than 3 dB.

Figure 7-28 shows similar data for two different row lengths. For these comparisons, the turbine spacing is constant and the row lengths are doubled by doubling the number of machines per row. When the receiver is at shorter distances, the predicted sound pressure levels are equal because of the equal turbine spacing. At longer distances, the levels for the double-length row are higher by 3 dB because the acoustic power per row is doubled.

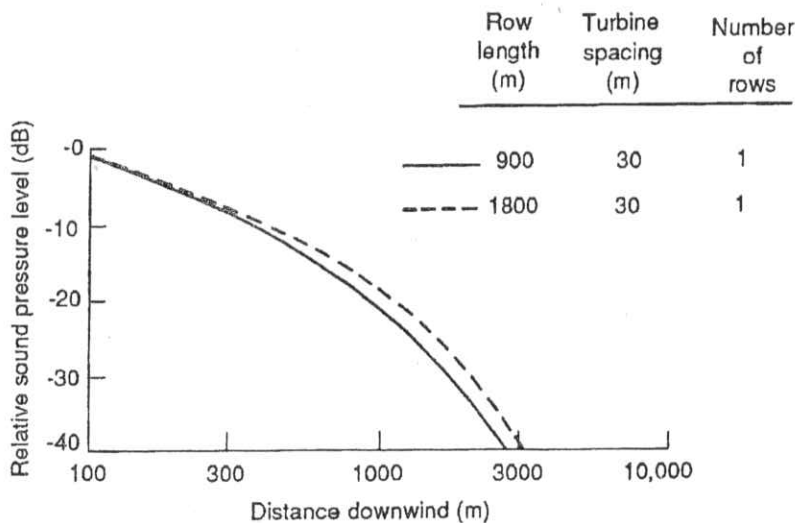


Figure 7-28. Calculated noise propagation downwind of wind turbines in rows of two different lengths ($\alpha = 0.54$ dB/100 m) [Shepherd and Hubbard 1986]

Computations were also made [Shepherd and Hubbard 1986] for a configuration similar to that of Figure 7-25, except that the row spacing was reduced from 200 m to 100 m. At all distances to the receiver, the computed sound pressure levels were higher for this more compact array.

Effect of Turbine Rated Power

Shepherd and Hubbard [1986] calculate the effect of the turbine's rated power on noise emissions by increasing the power of each turbine and the total station power. The turbine and row spacings were adjusted from those of Figure 7-25 to more appropriate values for larger machines (four times the rated power). Sound pressure levels from rows of 16 400-kW wind turbines were compared with levels from the same number of rows of 31 100-kW machines. This approximately doubled the rated power of the station. The reference spectrum for the larger turbines was assumed to have the same shape as that of the smaller turbines (Figure 7-10), although the levels were all 6 dB higher. This implies four times the acoustic power for four times the rated power. The computed sound pressure levels are 3 dB higher for the array of larger turbines because the acoustic power is doubled for each row of the array. Different results would be obtained if the reference spectra of the two sizes of turbines had different shapes.